JOURNAL OF CHEMICAL & ENGINEERING DATA

ARTICLE

pubs.acs.org/jced

Experimental Data on Phase Behavior of Simple Tetrabutylphosphonium Bromide (TBPB) and Mixed CO_2 + TBPB Semiclathrate Hydrates

Nadia Mayoufi,[†] Didier Dalmazzone,*[,†] Anthony Delahaye,[‡] Pascal Clain,[‡] Laurence Fournaison,[‡] and Walter Fürst[†]

[†]ENSTA ParisTech-UCP, 32 bd Victor, 75739 Paris Cedex 15, France

[‡]LGP2ES (EA 21), Cemagref-GPAN, Parc de Tourvoie BP 44, 92136 Antony Cedex, France

ABSTRACT: The phase behavior of simple and mixed semiclathrate hydrates formed from CO_2 + tetrabutylphosphonium bromide (TBPB) + water mixtures was investigated by pressure-controlled differential scanning calorimetry (DSC) at TBPB concentrations in the range of 0 to 0.073 mole fraction and at CO_2 pressure in the range of (0 to 2.0) MPa. In a previous article we demonstrated that TBPB + CO_2 mixed hydrates present high dissociation enthalpies and could be used as phase change material, covering the range of temperature from (284.6 to 289.0) K, for secondary refrigeration applications. The present work investigates a broader domain of compositions, resulting in $x-T$ phase diagrams at atmospheric conditions and at various CO_2 pressures. These data are required to model the potential latent heat of hydrate slurries as a function of gas pressure and aqueous phase composition over the whole range of interest for refrigeration purposes. The results presented show that adding TBPB to the water at low concentration (0.0058 mole fraction) decreases the pressure of formation of CO_2 hydrates to 0.5 MPa at 281.6 K, instead of 3.5 MPa at the same temperature in the absence of a promoter. Crystallization of CO_2 + TBPB hydrate could therefore offer an attractive means of capture for CO_2.

INTRODUCTION

Clathrate hydrates[1] are ice-like crystalline compounds in which small hydrophobic guest molecules, mostly light hydrocarbons, acid gases, or cyclic ethers, are physically trapped in host cavities shaped by a network of hydrogen-bonded water molecules. Under suitable pressure and temperature conditions, these structures are stabilized by van der Waals interactions between guest molecules and aqueous host cavities. Because of their annoying tendency to plug pipelines,[2] clathrate hydrates were considered for many years as the leading deepwater flow assurance problem in the energy industry.[3] Now, clathrate hydrates are also regarded favorably for various applications[4,5] as gas capture, storage, and transportation, and hydrates found in nature[6] may be potential sources of natural gas.

Semiclathrate hydrates[7−9] are very similar to clathrate hydrates, but the guest molecules in semiclathrate hydrates are organic salts composed of a peralkylonium cation physically trapped in the aqueous host cavity and anions (F^-, Cl^-, Br^-, NO_3^-, OH^-, etc.) inserted in the water network via hydrophilic interactions. Because of their suitable temperature and latent heat of melting,[10] semiclathrate hydrates of tetrabutylammonium bromide (TBAB) were first proposed as phase change materials (PCM) for cold storage and transportation in refrigeration and air-conditioning processes.[11,12] Semiclathrate hydrates were also studied for gas capture and storage applications since they have the capacity of hosting gases in free cavities present in their structures.[13] Several studies were thus carried out on mixed semiclathrate hydrates formed from various gases and peralkylonium salts.[14−22]

Mixed semiclathrate hydrates of CO_2 and peralkylonium salt were also proposed as new PCMs for cold storage and transportation in secondary refrigeration,[23,24] since their dissociation temperature may be varied with gas pressure and their dissociation enthalpy was higher than that of single peralkylonium salt semiclathrate hydrates. In fact, inserting gas molecules to form mixed hydrates generally stabilizes the structure, increasing both dissociation temperature and enthalpy. Such mixed hydrates formed with several additives could thus constitute a variety of efficient PCMs for thermal energy storage, with temperatures of transition adapted to various ranges of applications. As pointed out in our previous work,[24] mixed semiclathrate hydrates of CO_2 and tetrabutylphosphonium bromide (TBPB) formed from stoichiometric solutions have appropriate (p, T) stability conditions and latent heat content for secondary refrigeration applications.

The present work is complementary to this previous work,[24] since we present here experimental data on phase behavior of simple and mixed semiclathrate hydrates of CO_2 + TBPB formed from aqueous solutions at various TBPB mole fractions in the range of 0 to 0.073 and at various CO_2 pressures in the range of (0 to 2.0) MPa. Pressure-controlled differential scanning calorimetry (DSC) was used to investigate these systems. On the basis of the analysis of DSC results, we propose a discussion on the potential of semiclathrate-hydrate-based systems for a use in secondary refrigeration, but also for gas capture and storage applications.

APPARATUS AND MATERIALS

Materials. Analytical grade TBPB ([3115-68-2], 0.99 mass fraction) was purchased from Alpha Aesar and used with no

Received: April 21, 2011
Accepted: May 13, 2011
Published: May 24, 2011

dx.doi.org/10.1021/je2003918 | *J. Chem. Eng. Data* 2011, 56, 2987–2993

further purification. Freshly distilled water was carefully degassed before preparing 17 solutions in the range of composition of interest for semiclathrate investigation. Table 1 summarizes the compositions of these solutions, in which the range for salt mole fraction, x_{TBPB}, was 0.00276 to 0.07302. Corresponding mass fractions and H_2O/TBPB mole ratios are also reported in Table 1. N45 grade CO_2 (0.99995 mole fraction) was purchased from Air Liquide.

Table 1. Composition of the TBPB Solutions Used for the Measurements

TBPB concentration					
w_{TBPB}	x_{TBPB}	n_{H_2O}/n_{TBPB}	w_{TBPB}	x_{TBPB}	n_{H_2O}/n_{TBPB}
0.050	0.00276	361.8	0.330	0.02521	38.7
0.100	0.00580	171.4	0.344	0.02676	36.4
0.150	0.00918	107.9	0.371	0.02992	32.4
0.200	0.01296	76.2	0.400	0.03382	28.6
0.235	0.01588	62.0	0.430	0.03810	25.2
0.250	0.01720	57.1	0.450	0.04119	23.3
0.275	0.01953	50.2	0.500	0.04989	19.0
0.300	0.02201	44.4	0.600	0.07302	12.7
0.320	0.02412	40.5			

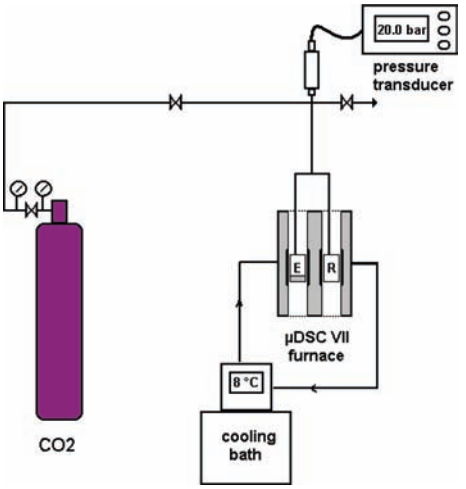

Figure 1. Experimental device. E: sample cell. R: reference cell.

HP-DSC Experimental Setup and Protocol. The experimental setup, illustrated in Figure 1, has been described previously.[24−26] It is based on a high sensitivity differential scanning calorimeter (micro DSC VII from Setaram, France) fitted with two pressure-controlled Hastelloy cells having a maximum operating pressure of 40 MPa. The feed gas cylinder was connected to the sample cell via a simple stage pressure regulator that allowed the working pressure to be adjusted from ambient pressure to 3 MPa. Pressure was measured by a Druck gauge within the range (0 to 3) MPa with a resolution of 0.001 MPa. The melting of high purity mercury and gallium samples was used to calibrate the DSC in the temperature range of interest, (230 to 300) K. Ice melting experiments performed to further control the calibration showed a measurement accuracy better than 1 % in enthalpy and 0.2 K in the phase change temperature.

A sample of solution of (50 to 60) mm^3 in volume, carefully weighed using a 10^{-5} g precision analytical balance, was inserted in the laboratory cell (E), while the reference cell (R) was left empty. The cells were then inserted into the furnace and connected to the gas feed line. A blank experiment was first performed at ambient pressure with no CO_2 added. Then, the sample cell was purged with CO_2 to evacuate the air, and CO_2 pressure was set to the desired value and kept constant during each determination. Increasing experimental pressures were successively applied, in the range (0.5 to 2) MPa. The temperature program consisted in a cooling sequence down to 243 K at the rate of 0.0333 $K \cdot s^{-1}$, an isotherm at 243 K for 20 min to allow sample crystallization, and a warming sequence up to 298 K at $8.333 \cdot 10^{-3}$ $K \cdot s^{-1}$ to melt the solids.

As crystallization of solid phases always requires subcooling and thus occurs out of equilibrium in DSC experiments, the determination of equilibrium points was realized using the melting heat flow curves upon slow warming. Phase change temperatures were measured according to the protocol that has

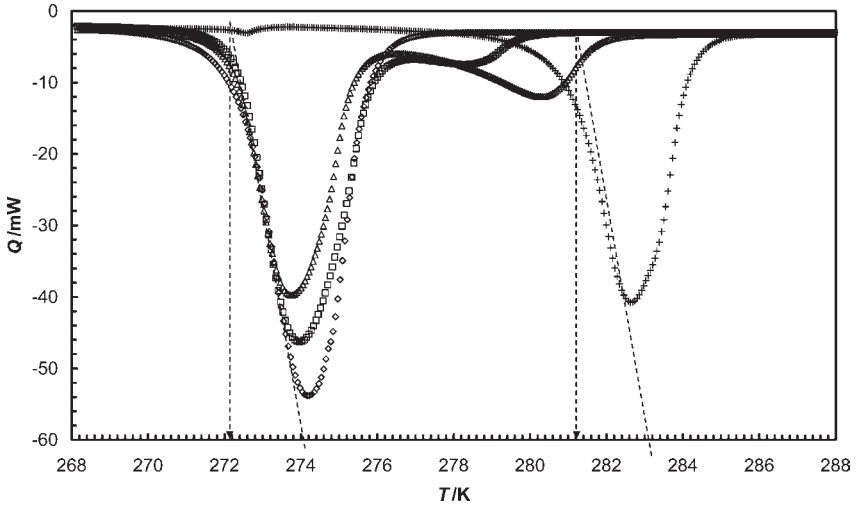

Figure 2. Heat flow, Q, versus temperature, T, obtained with TBPB solutions of variable mole fraction, x_{TBPB}: ◇, x_{TBPB} = 0.00276; □, x_{TBPB} = 0.00580; △, x_{TBPB} = 0.00918; +, x_{TBPB} = 0.02992. Dashed lines represent the tangent to invariant temperature melting peaks. Dashed arrows point the onset temperature (invariant peak) or the temperature of the end of fusion (progressive peak).

dx.doi.org/10.1021/je2003918 |J. Chem. Eng. Data 2011, 56, 2987–2993

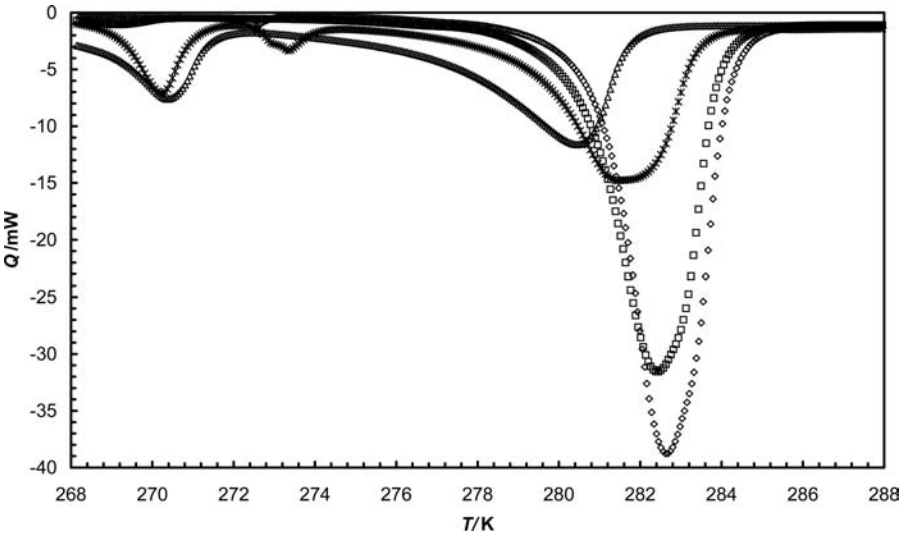

Figure 3. Heat flow, Q, versus temperature, T, obtained with TBPB solutions of variable mole fraction, x_{TBPB}: ◇, x_{TBPB} = 0.02992; □, x_{TBPB} = 0.03382; ∗, x_{TBPB} = 0.04989; △, x_{TBPB} = 0.07302.

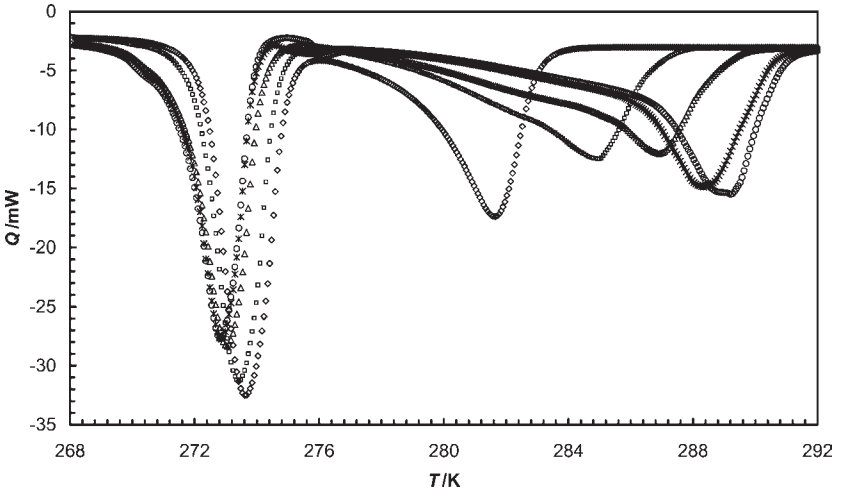

Figure 4. Heat flow, Q, versus temperature, T, obtained with a TBPB solution (x_{TBPB} = 0.01296) at variable CO_2 pressure, p_{CO_2}: ◇, p_{CO_2} = 0; □, p_{CO_2} = 0.5 MPa; △, p_{CO_2} = 1.0 MPa; ∗, p_{CO_2} = 1.5 MPa; ○, p_{CO_2} = 1.7 MPa.

been described in detail.[25−28] It has been demonstrated that using such a small sample volume and slow warming rate ensures a standard deviation of the measured temperature better than 0.2 K. The uncertainty will thus be stated as ± 0.4 K.

RESULTS AND DISCUSSION

Heat Flow Curves of Hydrate Dissociation in the TBPB + H_2O System. Figures 2 and 3 present heat flow curves versus temperature obtained upon warming after crystallizing the liquid samples without gas pressure. Only a part of the solutions that were studied in this work are presented in these figures for better legibility. Figure 2 corresponds to the TBPB mole fractions in water x_{TBPB} below 0.03, which is close to the composition of the hydrate TBPB·32H_2O (x_{TBPB} = 0.0303).[7] At lower concentrations, a first peak is attributed to the melting of a eutectic mixture of ice and TBPB·32H_2O, at a constant temperature of approximately 272.2 K. The excess TBPB·32H_2O hydrate then undergoes progressive melting. The dashed lines and arrows are presented as a reminder of the way of measuring equilibrium temperatures in DSC curves.[27,28] It can be seen from this figure that the determination of invariant temperatures of phase change, such as eutectic or pure compound melting, is achievable with good precision, while that of progressive melting is subject to larger uncertainties especially with broad peaks. The stated ± 0.4 K accuracy accounts for that uncertainty.

With the less concentrated solution sample (x_{TBPB} = 0.00276), only the eutectic melting is visible, which suggests that the composition of the eutectic mixture is very close to {0.003 TBPB + 0.997 H_2O}. At x_{TBPB} = 0.02992, which is close to the composition of the hydrate TBPB·32H_2O, the eutectic melting is barely visible.

Figure 3 corresponds to higher concentration samples. The main peak of each heat flow curve corresponds to the progressive melting of TBPB·32H_2O hydrate, ending at a temperature that decreases with increasing salt concentration. Another

dx.doi.org/10.1021/je2003918 |J. Chem. Eng. Data 2011, 56, 2987–2993

series of peaks is evidenced, having its onset at the constant temperature of 269.7 K. This denotes the presence of an invariant mixture formed from the TBPB·32H_2O hydrate and another solid that was not identified. The additional peak observed at 273 K with the sample at x_{TBPB} = 0.04989 is attributed to the melting of metastable ice, due to its onset temperature.

Heat Flow Curves of Hydrate Dissociation in the CO_2 + TBPB + H_2O System. Sample solutions were then submitted to the same temperature program in the presence of CO_2 at various pressures, ranging from (0.5 to 2) MPa. In most cases CO_2 pressures approaching 2 MPa caused the gas liquefaction in the cell during the cooling sequence, thus perturbing the measurement. We therefore limited the range of experimental pressure to 1.7 MPa in most experiments. Figures 4, 5, and 6 present the heat flow curves obtained at the various CO_2 pressures with solution samples of TBPB mole fractions equal to 0.01296, 0.02521 and 0.03382, respectively.

The first observation that arises from Figures 4 to 6 is that increasing CO_2 pressures increase the melting temperature of the hydrate and change the shape of the corresponding peak.

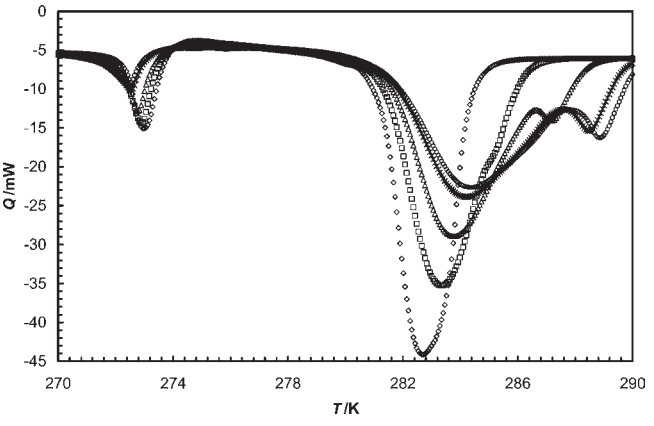

Figure 5. Heat flow, Q, versus temperature, T, obtained with a TBPB solution (x_{TBPB} = 0.02521) at variable CO_2 pressure, p_{CO_2}: ◇, p_{CO_2} = 0; □, p_{CO_2} = 0.5 MPa; △, p_{CO_2} = 1.0 MPa; ∗, p_{CO_2} = 1.5 MPa; ○, p_{CO_2} = 1.7 MPa.

At higher TBPB concentrations (Figure 5 and 6) an additional peak is clearly visible, demonstrating the formation of an additional, more stable, solid phase that we assume to be a mixed hydrate of TBPB and CO_2. The incomplete conversion of metastable single TBPB hydrate to stable mixed hydrate is due to the lack of mixing device in the DSC cells. The complete conversion in these conditions requires very long thermal cycling and is useful only for quantitative measurements. We previously presented determinations of dissociation enthalpies realized on mixed TBPB hydrates with H_2[22] and CO_2,[24] using such cycling experiments. For $p-T$ measurements this is not necessary since only a tiny amount of hydrates is sufficient to measure its dissociation temperature at a given pressure. It should be noticed however that in some cases the dissociation peak could not be distinguished. This is illustrated by Figure 6 for x_{TBPB} = 0.03382 at 0.5 MPa CO_2 pressure.

Phase Diagrams. Dissociation heat flow curves were then used to determine the temperature stability limits for single TBPB hydrates and mixed TBPB-CO_2 hydrates. The results obtained with all of the TBPB/H_2O solutions at various gas pressures are reported in Table 2. Missing values correspond to undistinguishable peaks as mentioned above.

The measured dissociation temperatures are presented in an $x-T$ diagram in Figure 7. The results obtained without CO_2 pressure may be compared with those of Dyadin and Udachin,[7] who first published the phase diagram of the TBPB−water binary system reproduced in Figure 8. Our measurements agree with the existence of a compound exhibiting congruent melting at approximately 281.2 K (282 K for ref 7) and which composition corresponds to TBPB·32H_2O. Although Dyadin and Udachin did not plot the ice + hydrate eutectic line on their diagram, it arises clearly from our DSC heat flow curves, with an invariant melting temperature of 272.2 K. Dyadin and Udachin[7] also mentioned the existence of a second, noncongruent melting hydrate TBPB·36H_2O and another metastable hydrate having lower melting temperatures. Our experiments did not allow confirming these additional phases.

As can be seen in Figure 7, the dissociation temperatures of TBPB semiclathrate hydrates are increased by (3.5 to 8) K in the presence of CO_2 atmosphere, depending on the pressure. Such stabilization can only be explained by the inclusion of gas into

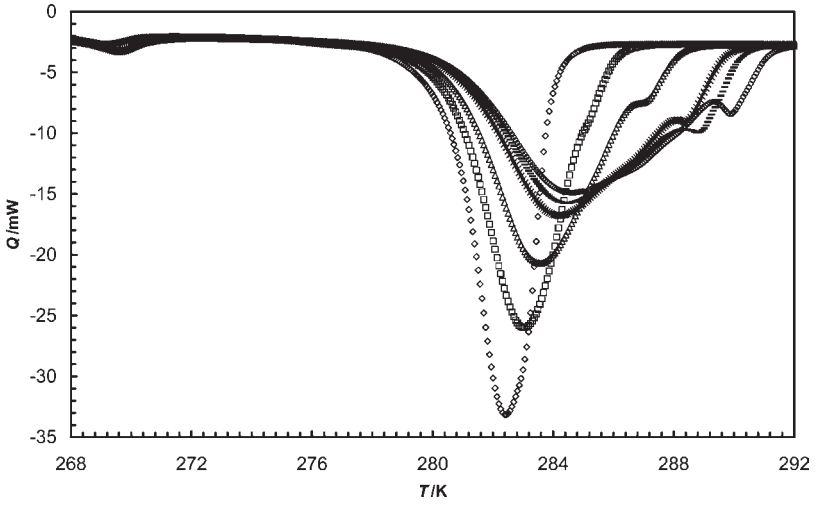

Figure 6. Heat flow, Q, versus temperature, T, obtained with a TBPB solution (x_{TBPB} = 0.03382) at variable CO_2 pressure, p_{CO_2}: ◇, p_{CO_2} = 0; □, p_{CO_2} = 0.5 MPa; △, p_{CO_2} = 1.0 MPa; ∗, p_{CO_2} = 1.5 MPa; —, p_{CO_2} = 1.7 MPa; ○, p_{CO_2} = 2.0 MPa.

dx.doi.org/10.1021/je2003918 |J. Chem. Eng. Data 2011, 56, 2987–2993

available cavities of the semiclathrate structure. Inserted CO_2 molecules interact with the aqueous lattice via van der Waals forces, thus increasing its thermodynamic stability, that is, its dissociation temperature and enthalpy.[24] This phenomenon, known as gas enclathration, has been observed on many gaseous species with a variety of similar hydrates formed from tetrabutylammonium fluoride, chloride, bromide, and others.[13−24]

Table 2. Dissociation Temperatures, T_{diss} (Accuracy of ± 0.4), of Single TBPB Semiclathrate Hydrates and Mixed CO_2 + TBPB Semiclathrate Hydrates at CO_2 Pressures, p_{CO_2}, from (0 to 1.7) MPa for TBPB Mole Fractions, x_{TBPB}, from 0.00276 to 0.07302

	p_{CO_2}/MPa					
x_{TBPB}	0		0.5	1.0	1.5	1.7
	T_{diss}/K					
	Eutectic	TBPB Hydrate	Mixed TBPB + CO_2 Hydrate			
0.00276	272.2	272.2	273.8			
0.00580	272.3	278.0	281.6	284.6	286.0	286.7
0.00918	272.1	279.8	283.3	286.1	287.4	288.0
0.01296	272.2	280.5		286.6	287.9	288.3
0.01588	272.2	280.8	284.3	286.7	287.9	288.3
0.01720	272.1	280.9		286.8	288.0	288.4
0.01953	272.2	281.0	284.5	286.8	288.1	288.4
0.02201	272.3	281.1	284.5	286.9	288.2	288.5
0.02412	272.2	281.1	284.6	286.9	288.2	288.5
0.02521	272.1	281.2	284.6	286.9	288.2	288.5
0.02676	272.2	281.2		286.9	288.1	288.5
0.02992	272.2	281.2	284.6	286.9	288.2	288.5
0.03382		281.1		286.8	287.9	288.3
0.03810		281.0	284.5	286.5	287.6	288.1
0.04119		280.9	284.3	286.3	287.4	288.0
0.04989		280.6	283.9	285.7	286.8	287.4
0.07302		279.5	282.9	284.6	285.6	286.2

For refrigeration purposes, the knowledge of the phase diagrams presented in Figure 7 is essential to model the solid fraction of hydrate slurries formed from solutions of variable composition at variable CO_2 pressure. These data can be used in complement of the dissociation enthalpies reported in previous work[24] to determine the latent heat content of such slurry and, thus, its efficiency for cold storage and transportation applications.[29]

Figure 9 reports hydrate−liquid−vapor (p, T) equilibrium points for the systems CO_2 + H_2O, from literature,[30,31] and TBPB + H_2O and CO_2 + TBPB + H_2O, from the present work. In comparison with simple CO_2 clathrate hydrates, mixed TBPB + CO_2 semiclathrate hydrates present increased temperature stability limits, by (11 to 13) K at a given pressure depending on the salt concentration. At temperatures within the range (281 to 284) K, the pressures of formation of the mixed hydrates are much lower than that of simple CO_2 hydrates. For instance, the pressure limit of hydrate stability is 0.5 MPa at 281.6 K in CO_2 + TBPB + H_2O with x_{TBPB} = 0.00580, instead of 3.475 MPa at 281.5 K in CO_2 + H_2O.[30] With x_{TBPB} = 0.00918, it is 0.5 MPa at 283.3 K instead of 4.468 MPa at the same temperature without TBPB.

Previous studies[24] demonstrated that TBAB and TBPB at concentrations corresponding to the semiclathrates' stoichiometry

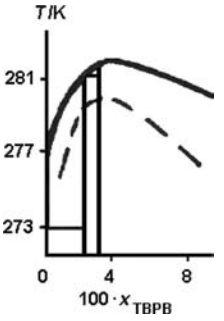

Figure 8. Temperature phase boundaries, T, versus TBPB mole fraction, x_{TBPB}, in the TBPB + H_2O phase diagram by Dyadin and Udachin.[7]

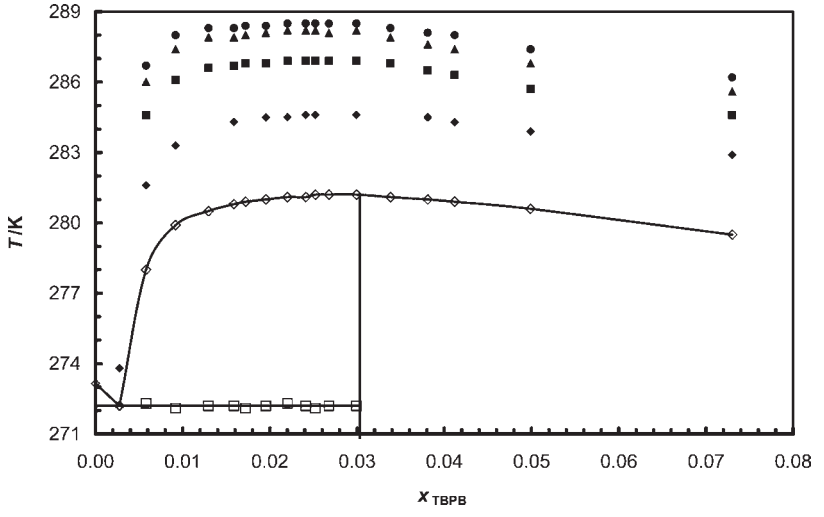

Figure 7. Temperature phase boundaries, T, versus TBPB mole fraction, x_{TBPB}, in the binary system TBPB + H_2O and in the ternary system CO_2 + TBPB + H_2O at variable CO_2 pressure, p_{CO_2}. TBPB + H_2O: ◇, liquidus; □, eutectic. CO_2 + TBPB + H_2O: ♦, p_{CO_2} = 0.5 MPa; ■, p_{CO_2} = 1 MPa; ▲, p_{CO_2} = 1.5 MPa; ●, p_{CO_2} = 1.7 MPa.

dx.doi.org/10.1021/je2003918 |J. Chem. Eng. Data 2011, 56, 2987–2993

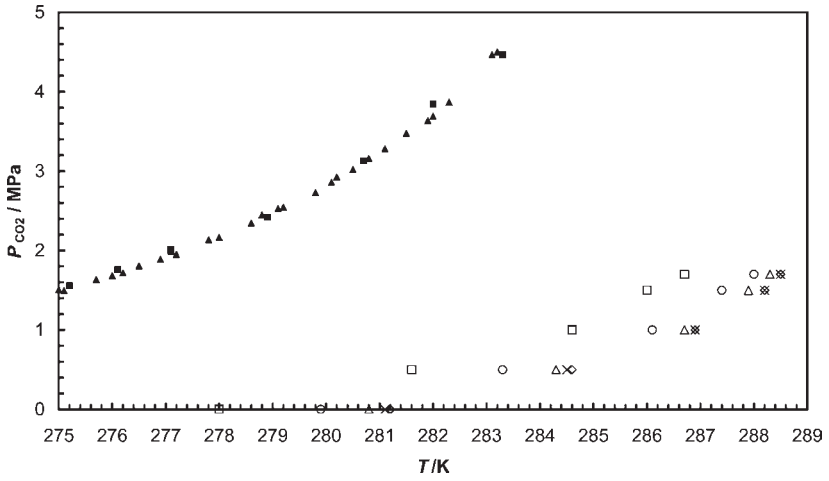

Figure 9. CO_2 pressure, p_{CO_2}, versus temperature, T, H−L−V equilibrium data for the systems $CO_2 + H_2O$ (literature) and $CO_2 + TBPB + H_2O$ (present work). $CO_2 + H_2O$: ▲, Larson;[30] ■, Robinson and Mehta.[31] $CO_2 + TBPB + H_2O$ at various TBPB mole fractions, x_{TBPB}: □, x_{TBPB} = 0.00580; ○, x_{TBPB} = 0.00918; △, x_{TBPB} = 0.01588; ×, x_{TBPB} = 0.02201; ◇, x_{TBPB} = 0.02992.

($TBAB \cdot 26H_2O$ and $TBPB \cdot 32H_2O$, respectively) have comparable stabilizing effects on CO_2 hydrates. The results presented in Figure 9 show that TBPB presents a high stabilizing efficiency at mole fractions as low as 0.0058. This is very interesting for cold storage and transportation applications, which generally requires low operating pressures. Moreover, this is of great interest for an application to CO_2 removal from flue gas, since one of the main sources of operational expenses in such a process is expected to be the compression work required to bring the CO_2 at a partial pressure sufficient to form hydrates. For that purpose, similar promoters such as TBAB have been considered for lowering the pressure of formation of CO_2 hydrates.[32] According to Arjmandi et al.,[13] the pressure-reducing effect of TBAB is of the same order of magnitude than that we have found for TBPB, although the two studies do not concern the same pressure range. For example, dissociation temperatures of mixed TBAB + CO_2 hydrates formed from a low concentration solution (x_{TBAB} = 0.00620) were from 285.55 K at 1.4 MPa to 289.25 K at 4.09 MPa.[13] With a comparable concentration of TBPB (x_{TBPB} = 0.00580) we obtained mixed hydrates that dissociate in the range of 281.6 K at 0.5 MPa to 286.7 K at 1.7 MPa. Besides thermodynamic stability, other properties will control the efficiency of a hydrate-based CO_2 removal process. First, the amount of gas entrapped in a given mass of semiclathrate is of primary importance because the energy of hydrate formation and dissociation is mainly related to the aqueous network formation and destruction, thus poorly dependent on the gas content. We previously reported that the dissociation enthalpies of TBPB hydrate and TBAB hydrate, when expressed on a Joule-per-H_2O-mole basis, are very close. Also, the gas occupancy in terms of mole of CO_2 per mole of H_2O appears to be significantly higher in TBPB hydrates than in other similar semiclathrates.[24] In other words, the energy required to form and dissociate the hydrates is lower, on a Joule-per-CO_2-mole basis for TBPB-enhanced hydrates than with other similar promoters. From the point of view of energy consumption, TBPB is thus likely to provide a competitive solution as a promoter for a hydrate-based CO_2 capture process. Another key property for assessing the efficiency of such process is the selectivity. Does the hydrate have the capability of concentrating CO_2 and rejecting the other gases present in the mixture to be treated? This point requires quantitative analysis of the hydrate composition, which is beyond the scope of the present work.

CONCLUSIONS

The phase behavior in the systems TBPB + water and TBPB + carbon dioxide + water was investigated using pressure-controlled DSC. The dissociation temperatures of TBPB semiclathrate hydrates formed from aqueous TBPB solutions of various mole fractions in the range (0.0028 to 0.0730) were measured, and the resulting $x-T$ phase diagram for the TBPB + H_2O binary system was found to be in agreement with literature. CO_2 insertion has a strong stabilizing effect on the semiclathrate structure, with an average increase of the dissociation temperature ranging from 3.5 K at 0.5 MPa CO_2 pressure to 8 K at 1.7 MPa, over the whole domain of concentration investigated.

These results will be useful for characterizing the solid content of mixed TBPB-CO_2 hydrate slurries formed at various $p-T-x$ conditions. Used in association with the dissociation enthalpies presented in a previous article, they will serve to establish the useable latent heat of the slurry for cold storage and transportation purposes.

In addition, a TBPB mole fraction as low as 0.006 in the water phase is sufficient to lower the pressure limit of stability of CO_2-containing hydrates from (3.5 to 0.5) MPa at 281.6 K. Mixed TBPB + CO_2 hydrates are therefore a potential solution for hydrate-based processes in the fields of refrigeration and CO_2 capture.

AUTHOR INFORMATION

Corresponding Author

*E-mail: didier.dalmazzone@ensta-paristech.fr. Tel.: +33 1 45 52 63 16.

Funding Sources

The ADEME is acknowledged for financial support (Contract No. 05 74 C 0013).

REFERENCES

(1) Sloan, E. D. *Clathrate Hydrate of Natural Gases*; Marcel Dekker Inc.: New York, 1998.

(2) Hammerschmidt, E. G. Formation of Gas Hydrates in Natural Gas Transmission Lines. *Ind. Eng. Chem.* **1934**, *26*, 851–855.
(3) Sloan, E. D. A changing hydrate paradigm--from apprehension to avoidance to risk management. *Fluid Phase Equilib.* **2005**, *228*−*229*, 67–74.
(4) Chatti, I.; Delahaye, A.; Fournaison, L.; Petitet, J.-P. Benefits and drawbacks of clathrate hydrates: a review of their areas of interest. *Energy Convers. Manage.* **2005**, *46*, 1333–1343.
(5) Englezos, P. Clathrate Hydrates. *Ind. Eng. Chem. Res.* **1993**, *32*, 1251–1274.
(6) Kvenvolden, K. A. Natural gas hydrate occurrence and issues. *Ann. N.Y. Acad. Soc.* **1994**, *715*, 232–246.
(7) Dyadin, Y. A.; Udachin, K. A. Clathrate formation in water-peralkylonium salts systems. *J. Inclusion Phenom.* **1984**, *2*, 61–72.
(8) Fowler, D. L.; Loebenstein, W. V.; Pall, D. B.; Kraus, C. A. Some Unusual Hydrates of Quaternary Ammonium Salts. *J. Am. Chem. Soc.* **1940**, *62*, 1140–1142.
(9) Jeffrey, G. A.; McMullan, R. K. *Progress in Inorganic Chemistry*; John Wiley: New York, 1967; Vol. 8, pp 43−108.
(10) Oyama, H.; Shimada, W.; Ebinuma, T.; Kamata, Y.; Takeya, S.; Uchida, T.; Nagao, J.; Narita, H. Phase Diagram, Latent Heat, and Specific Heat of TBAB Semiclathrate Hydrate Crystals. *Fluid Phase Equilib.* **2005**, *234*, 131–135.
(11) Fukushima, S.; Takao, S.; Ogoshi, H.; Ida, H.; Matsumoto, S.; Akiyama, T.; Otsuka, T. Development of high-density cold latent heat with clathrate hydrate. *NKK Tech. Rep.* **1999**, *166*, 65–70.
(12) Tanasawa, I.; Takao, S. Low-Temperature Storage Using Clathrate Hydrate Slurries of Tetra-n-butylammonium Bromide: Thermophysical Properties and Morphology of Clathrate Hydrate Crystals, *4th International Conference on Gas Hydrates*, Yokohama, Japan, May 19−23, 2002; pp 963−967.
(13) Arjmandi, M.; Chapoy, A.; Tohidi, B. Equilibrium Data of Hydrogen, Methane, Nitrogen, Carbon Dioxide, and Natural Gas in Semi-Clathrate Hydrates of Tetrabutyl Ammonium Bromide. *J. Chem. Eng. Data* **2007**, *52*, 2153–2158.
(14) Chapoy, A.; Anderson, R.; Tohidi, B. Low-Pressure Molecular Hydrogen Storage in Semi-clathrate Hydrates of Quaternary Ammonium Compounds. *J. Am. Chem. Soc.* **2007**, *129*, 746–747.
(15) Fan, S.; Li, S.; Wang, J.; Lang, X.; Wang, Y. Efficient Capture of CO_2 from Simulated Flue Gas by Formation of TBAB or TBAF Semiclathrate Hydrates. *Energy Fuels* **2009**, *23*, 4202–4208.
(16) Hashimoto, S.; Sugahara, T.; Moritoki, M.; Sato, H.; Ohgaki, K. Thermodynamic stability of hydrogen + tetra-n-butyl ammonium bromide mixed gas hydrate in nonstoichiometric aqueous solutions. *Chem. Eng. Sci.* **2008**, *63*, 1092–1097.
(17) Li, D.-L.; Du, J.-W.; Fan, S.-S.; Liang, D.-Q.; Li, X.-S.; Huang, N.-S. Clathrate Dissociation Conditions for Methane + Tetra-n-butyl Ammonium Bromide (TBAB) + Water. *J. Chem. Eng. Data* **2007**, *52*, 1916–1918.
(18) Li, S.; Fan, S.; Wang, J.; Lang, X.; Liang, D. CO_2 capture from binary mixture via forming hydrate with the help of tetra-n-butyl ammonium bromide. *J. Nat. Gas Chem.* **2009**, *18*, 15–20.
(19) Sakamoto, J.; Hashimoto, S.; Tsuda, T.; Sugahara, T.; Inoue, Y.; Ohgaki, K. Thermodynamic and Raman spectroscopic studies on hydrogen + tetra-n-butyl ammonium fluoride semi-clathrate hydrates. *Chem. Eng. Sci.* **2008**, *63*, 5789–5794.
(20) Makino, T.; Yamamoto, T.; Nagata, K.; Sakamoto, H.; Hashimoto, S.; Sugahara, T.; Ohgaki, K. Thermodynamic Stabilities of Tetra-n-butyl Ammonium Chloride + H_2, N_2, CH_4, CO_2, or C_2H_6 Semiclathrate Hydrate Systems. *J. Chem. Eng. Data* **2010**, *55*, 839–841.
(21) Deschamps, J.; Dalmazzone, D. Dissociation enthalpies and phase equilibrium for TBAB semi-clathrate hydrates of N_2, CO_2, N_2 + CO_2 and CH_4 + CO_2. *J. Therm. Anal. Calorim.* **2009**, *98*, 113–118.
(22) Deschamps, J.; Dalmazzone, D. Hydrogen Storage in Semi-clathrate Hydrates of Tetrabutyl Ammonium Chloride and Tetrabutyl Phosphonium Bromide. *J. Chem. Eng. Data* **2010**, *55*, 3395–3399.
(23) Lin, W.; Delahaye, A.; Fournaison, L. Phase equilibrium and dissociation enthalpy for semi-clathrate hydrate of CO_2 + TBAB. *Fluid Phase Equilib.* **2008**, *264*, 220–227.
(24) Mayoufi, N.; Dalmazzone, D.; Fürst, W.; Delahaye, A.; Fournaison, L. CO_2 Enclathration in Hydrates of Peralkyl-(Ammonium/Phosphonium) Salts: Stability Conditions and Dissociation Enthalpies. *J. Chem. Eng. Data* **2010**, *55*, 1271–1275.
(25) Delahaye, A.; Fournaison, L.; Marinhas, S.; Chatti, I.; Petitet, J.-P.; Dalmazzone, D.; Fürst, W. Effect of THF on equilibrium pressure and dissociation enthalpy of CO_2 hydrates applied to secondary refrigeration. *Ind. Eng. Chem. Res.* **2006**, *45*, 391–397.
(26) Martínez, M. C.; Dalmazzone, D.; Fürst, W.; Delahaye, A.; Fournaison, L. Thermodynamic properties of THF + CO_2 hydrates in relation with refrigeration applications. *AIChE J.* **2008**, *54*, 1088–1095.
(27) Kharrat, M.; Dalmazzone, D. Experimental Determination of Stability Conditions of Methane Hydrate in Aqueous Calcium Chloride Solutions Using High Pressure Differential Scanning Calorimetry. *J. Chem. Thermodyn.* **2003**, *35*, 1489–1505.
(28) Dalmazzone, D.; Clausse, D.; Dalmazzone, C.; Herzhaft, B. The stability of methane hydrates in highly concentrated electrolyte solutions by differential scanning calorimetry and theoretical computation. *Am. Miner.* **2004**, *89*, 1183–1191.
(29) Marinhas, S.; Delahaye, A.; Fournaison, L.; Dalmazzone, D.; Fürst, W.; Petitet, J.-P. Modelling of the available latent heat of a CO_2 hydrate slurry in an experimental loop applied to secondary refrigeration. *Chem. Eng. Process.* **2006**, *45*, 184–192.
(30) Larson, S. D. Phase studies of the two-components carbon dioxide-water system, involving the carbon dioxide hydrate. Ph.D. Thesis, University of Illinois, Urbana, IL, 1955.
(31) Robinson, D. B.; Mehta, B. R. Hydrates in the propane-carbon dioxide-water system. *J. Can. Pet. Technol.* **1971**, *10*, 33–36.
(32) Duc, N. H.; Chauvy, S.; Herri, J.-M. CO_2 capture by hydrate crystallization—A potential solution for gas emission of steelmaking industry. *Energy Convers. Manage.* **2007**, *48*, 1313–1322.